Experimental study of the low-lying structure of ^{94}Zr with the $(n, n'\gamma)$ reaction

E. Elhami,[1] J. N. Orce,[1,*] M. Scheck,[1] S. Mukhopadhyay,[1] S. N. Choudry,[1] M. T. McEllistrem,[1] S. W. Yates,[1,2] C. Angell,[3,4] M. Boswell,[3,4] B. Fallin,[4,5] C. R. Howell,[4,5] A. Hutcheson,[4,5] H. J. Karwowski,[3,4] J. H. Kelley,[4,6] Y. Parpottas,[4,5] A. P. Tonchev,[4,5] and W. Tornow[4,5]

[1]*Department of Physics & Astronomy, University of Kentucky, Lexington, Kentucky 40506-0055, USA*
[2]*Department of Chemistry, University of Kentucky, Lexington, Kentucky 40506-0055, USA*
[3]*Department of Physics & Astronomy, University of North Carolina, Chapel Hill, North Carolina 27599-3255, USA*
[4]*Triangle Universities Nuclear Laboratory (TUNL), Durham, North Carolina 27708, USA*
[5]*Department of Physics, Duke University, Durham, North Carolina 27708-0308, USA*
[6]*Department of Physics, North Carolina State University, Raleigh, North Carolina 27695-8202, USA*

(Received 21 August 2008; published 10 December 2008)

The low-lying structure of $^{94}_{40}$Zr was studied with the $(n, n'\gamma)$ reaction, and a level scheme was established based on excitation function and $\gamma\gamma$ coincidence measurements. Branching ratios, multipole mixing ratios, and spin assignments were determined from angular distribution measurements. Lifetimes of levels up to 3.4 MeV were measured by the Doppler-shift attenuation method, and for many transitions the reduced transition probabilities were determined. In addition to the anomalous 2^+_2 state, which has a larger $B(E2; 2^+_2 \rightarrow 0^+_1)$ value than the $B(E2; 2^+_1 \rightarrow 0^+_1)$, the experimental results revealed interesting and unusual properties of the low-lying states in ^{94}Zr. In a simple interpretation, the excited states are classified in two distinct categories, i.e., those populating the 2^+_2 state and those decaying to the 2^+_1 state.

DOI: 10.1103/PhysRevC.78.064303 PACS number(s): 21.10.Re, 21.10.Tg, 25.40.Fq, 27.60.+j

I. INTRODUCTION

The nuclear structure of the even-A zirconium isotopes, as shown in Fig. 1, evolves from spherical, ^{90}Zr$_{50}$, to the strongly deformed nucleus ^{102}Zr [1–5], with a subshell closure at $N = 56$ for ^{96}Zr [3] and evidence of shape coexistence in ^{100}Zr [4]. This evolution is evinced by the $B(E2; 2^+_1 \rightarrow 0^+_1)$ values as well as the 2^+_1 excitation energies. In comparison to other Zr isotopes, the level scheme of ^{94}Zr is most similar to that of ^{92}Zr, and it is expected that the low-lying excited states in ^{94}Zr would exhibit somewhat vibrational character.

The original motivation for our study of the low-lying states in ^{94}Zr was the experimental identification of multiphonon symmetric and mixed-symmetry excitations, such as those seen in ^{94}Mo [6,7]. The mixed-symmetry (MS) states predicted by the IBM-2 model [8] are excitations whose wave functions are not fully symmetric with respect to the exchange of valence protons (π) and valence neutrons (ν), when π and ν are considered as additional degrees of freedom. For a spherical nucleus near a closed shell, it is predicted that the lowest-lying MS state has $J^\pi = 2^+$ and lies at $\sim$2 MeV excitation energy. Typical experimental signatures of a MS state are a magnetic dipole, $M1$, transition to the corresponding symmetric state with a $B(M1) \approx 1\ \mu^2_N$ and a weak $E2$ transition to the ground state with a $B(E2)$ of at most a few single-particle units [9]. Symmetric or MS multiphonon excitations arise from the $Q_{(\pi,\nu)}$-phonon couplings, as described in the Q-phonon scheme [10,11]; therefore, these excitations could be considered as the building blocks of the low-lying states in nearly spherical nuclei.

Multiphonon excitations have been observed experimentally in ^{94}Mo [6,7] and other $N = 52$ isotones, ^{96}Ru [12,13] and ^{92}Zr [14]. For the first time in an odd-A nucleus, ^{93}Nb, one-phonon MS states have been identified [15]. These experimental results have been confirmed by extensive shell model [13–16], quasiparticle phonon model (QPM), and IBM-2 [17,18] calculations, and are summarized, along with other examples in other regions of the nuclear chart, in a recent review by Pietralla *et al.* [19]. A much smaller $B(M1; 2^+_{1,\mathrm{ms}} \rightarrow 2^+_{1,s})$ value than that in ^{94}Mo has been observed in ^{96}Mo [20]. The question of how MS states evolve in this region can be addressed by studying ^{94}Zr, another $N = 54$ isotone.

Even though ^{94}Zr has been studied with many different probes (Ref. [21,22] and references therein), information on transition strengths is scarce. The available experimental data on the low-lying states in ^{94}Zr are limited to lifetimes for the first three excited levels, 2^+_1, 0^+_2, 4^+_1 and multipole mixing ratios for a few transitions [21]. In an earlier ^{94}Zr$(n, n'\gamma)$ measurement at the University of Kentucky by Glasgow and coworkers [23], no information on lifetimes was obtained. In our study, the Doppler-shift attenuation method (DSAM) was employed to determine the lifetimes of low-lying levels. With the lifetimes and other spectroscopic information, i.e., branching ratios and multipole mixing ratios, reduced transition probabilities have been determined to identify the one-phonon state and possibly members of the two-phonon MS states, as well as other collective excitations.

In our previous publication [24], we reported the results of an ^{94}Zr$(n, n'\gamma)$ angular distribution measurement at $E_n = 2.3$ MeV. In that report, we identified the 2^+_2 state at 1671.4 keV as the one-phonon MS state, 2^+_{ms} and commented on its anomalous behavior. The 752.5-keV $M1$ transition $(2^+_{\mathrm{ms}} \rightarrow 2^+_1)$ has $B(M1) = 0.31(3)\ \mu^2_N$, but the $E2$ transition to the ground-state results in $B(E2; 2^+_{\mathrm{ms}} \rightarrow 0^+_1) = 7.8(7)$ W.u.

*jnorce@triumf.ca

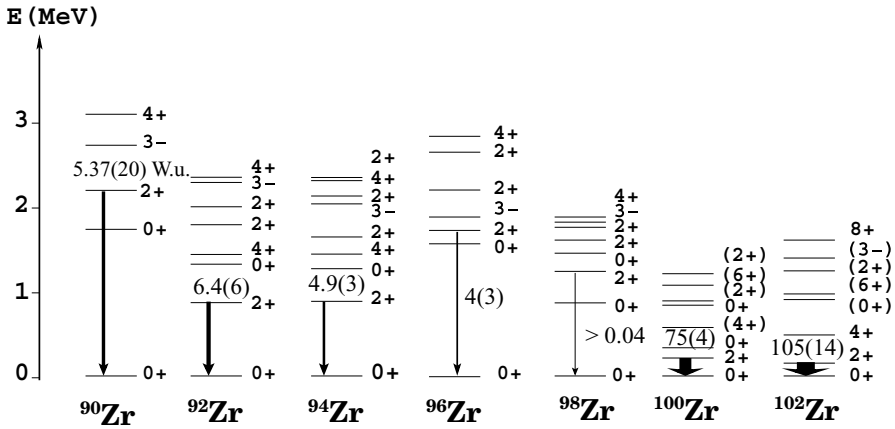

FIG. 1. Evolution of nuclear structure in even-A Zr isotopes. The data are from Ref. [22].

This latter value is unusually large for a one-phonon MS state decaying to the ground state and is larger than the $B(E2; 2_1^+ \rightarrow 0_1^+)$ value of 4.9(3) W.u. The $B(E2)$ and $B(M1; 2_{\rm ms}^+ \rightarrow 2_1^+)$ values for the neighboring nuclei are listed in Table I. The present study of the low-lying states in ^{94}Zr reveals an interesting and puzzling decay behavior, conveying a unique structural picture for this nucleus.

In this article, we present the results of the angular distribution measurements at $E_n = 2.3$, 2.8, and 3.5 MeV, an excitation function, and $\gamma\gamma$ coincidence measurements. The experimental methods are described in Sec. II, and the results are provided in Sec. III, which also includes a discussion of the level scheme. An interpretation of the level scheme is presented in Sec. IV, along with shell-model calculations. Our conclusions are drawn in Sec. V.

II. EXPERIMENTAL METHODS

A. Experiments at the University of Kentucky

The low-lying structure of ^{94}Zr was studied with the inelastic neutron scattering (INS), i.e., the $(n, n'\gamma)$ reaction [25]. Nearly monoenergetic fast neutrons were provided by the 7-MV electrostatic accelerator through the ^{3}H$(p, n)^3$He reaction. The gas target cell of 1.6 cm^3, which contained up to 1.0 atm of tritium gas, was isolated from the beam line vacuum by a 3.5-μm molybdenum foil. The pulsed beam of protons, at 533-ns intervals, bunched to about 1 ns, and a 2-μA current was delivered to the gas cell, producing a typical neutron flux of $\approx 10^6$ neutrons cm^{-2} s^{-1} at 5 cm from the gas cell, with $\Delta E \approx 60$ keV (at $E_n = 2.0$ MeV).

The scattering sample consisted of 20.03 g of ZrO_2 powder, enriched to 98.6% in ^{94}Zr, in a cylindrical vessel (2.6 cm $\times$ 3.9 cm), and it was suspended at 5 cm from the end of the gas cell. The γ rays produced by the $(n, n'\gamma)$ reaction were detected by a HPGe detector with 55% efficiency and a full width at half maximum (FWHM) of 1.8 keV at 1.33 MeV. The detector, surrounded by an annular BGO scintillator as an active Compton-suppression shield, was placed at a distance of 115 cm from the scattering sample. The detection assembly was protected from direct neutrons and background radiation by a tungsten wedge, shielding bodies of copper and boron-loaded polyethylene, with inserted lead rings. The time-of-flight technique was employed for further background suppression, where a gate was applied to record only beam-correlated γ-ray events, i.e., the prompt spectrum, and reject the noncorrelated events. The delayed events were recorded as a background spectrum. Figure 2 shows a typical γ-ray spectrum produced in the ^{94}Zr$(n, n'\gamma)$ measurements.

The $(n, n'\gamma)$ singles measurements included excitation functions and angular distributions. The excitation function measurements were carried out at incident neutron energies from 2.5 to 4.0 MeV in 100-keV intervals, with the detector at 90° with respect to the beam line. The angular distribution

TABLE I. Characteristics of the one-phonon symmetric and MS states in $N = 52$ and 54 nuclei.

Nucleus	$E_{\rm lev}$, J_i^π (keV)	$B(M1; 2_{\rm ms}^+ \rightarrow 2_1^+)$ (μ_N^2)	$B(E2; 2_i^+ \rightarrow 0_1^+)$ (W.u.)	Reference
$^{96}_{44}$Ru$_{52}$	832.6(1), 2_1^+		18.1(5)	
	2284.2(3), 2_3^+	0.78(23)	1.6(3)	[12]
$^{94}_{42}$Mo$_{52}$	871.09(10), 2_1^+		16(1)	
	2067.4(1), 2_3^+	0.56(5)	1.8(2)	[7]
$^{92}_{40}$Zr$_{52}$	934.46(10), 2_1^+		$6.4^{+0.6}_{-0.5}$	
	1847.3(1), 2_2^+	0.37(4)	3.4(4)	[14]
$^{96}_{42}$Mo$_{54}$	778.22(5), 2_1^+		20.7(3)	
	2095.73(5), 2_4^+	0.17(2)	$0.08^{+0.02}_{-0.01}$	[20]
$^{94}_{40}$Zr$_{54}$	918.80(10), 2_1^+		4.9(3)	[21]
	1671.40(10), 2_2^+	0.31(3)	7.8(7)	Present work

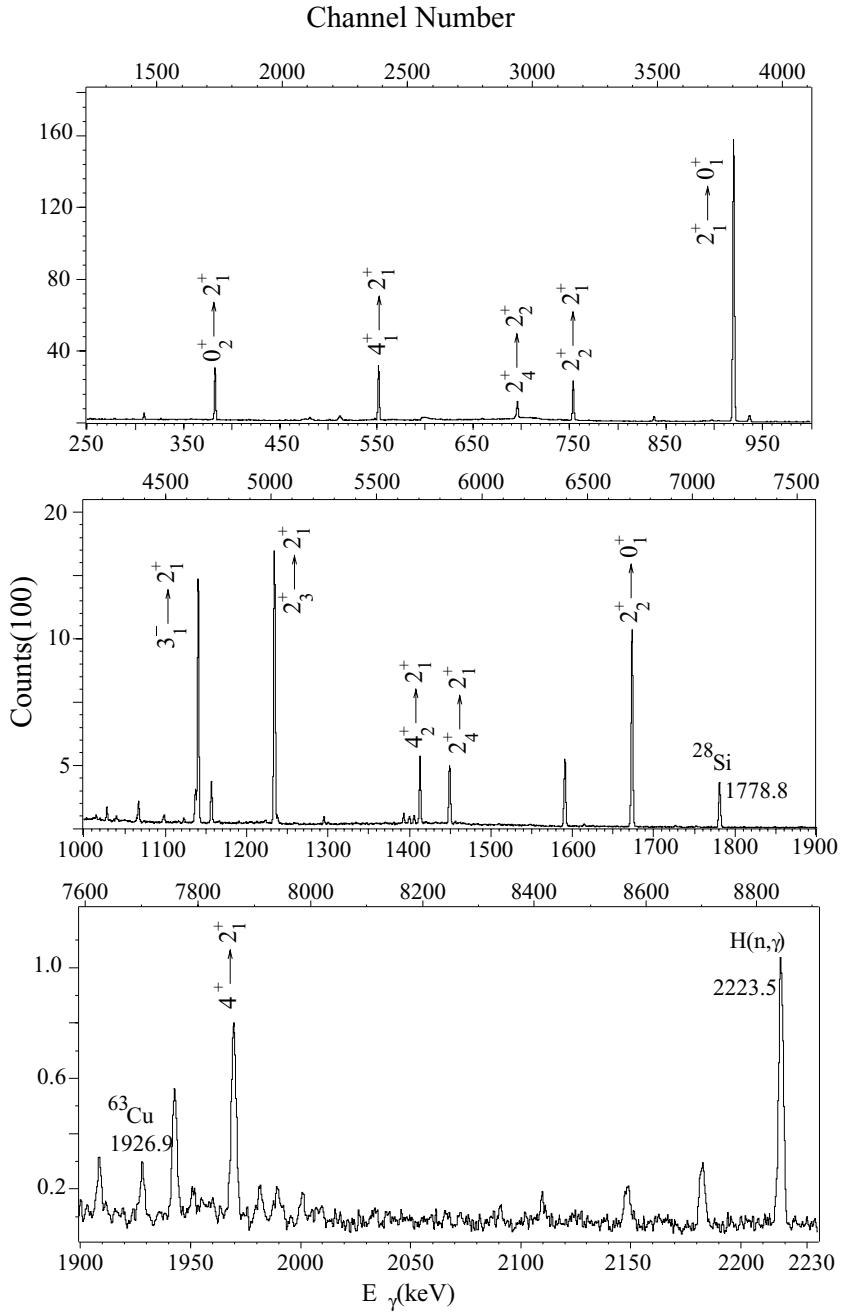

FIG. 2. γ-ray spectrum obtained from the ^{94}Zr$(n, n'\gamma)$ reaction at $E_n = 3.5$ MeV.

measurements were performed at three different neutron energies, $E_n = 2.3$, 2.8, and 3.5 MeV, for a range of detection angles, 40° to 150°, in approximately 10° steps. The level lifetimes and spin assignments along with branching ratio and multipole mixing ratios, δ, were determined from the angular distribution measurements.

B. Experiments at Triangle Universities Nuclear Laboratory

The $\gamma\gamma$ coincidence measurements were performed at the Triangle Universities Nuclear Laboratory (TUNL) at Duke University. Fast neutrons of 5.0 MeV were produced by the 10-MV FN Tandem Van de Graaff accelerator through the ^{2}H$(d, n)^3$He reaction. The 3.15-cm-long gas cell, filled with 5.0 atm of deuterium gas, was isolated from the beam line with a 6.35-μm Havar foil window. The experiment was performed at the shielded neutron source area, where the gas cell is mounted at the end of the 20° beam line. The specifics of the shielding area are described in Ref. [26] and schematically shown in Fig. 3.

Three HPGe clover detectors, each equipped with a BGO Compton suppression shield, were used to record the coincident events. The relative efficiency of each clover, consisting of four quadrants, was 4 × 22% with a FWHM of 2.25 keV for each quadrant at 1.33 MeV. The scattering sample, in a 2.6 cm × 3.9 cm cylindrical vessel, consisted of 20.45 g of ZrO_2 powder enriched to 98.6% in ^{94}Zr and was suspended at 214 cm from the shielding wall.

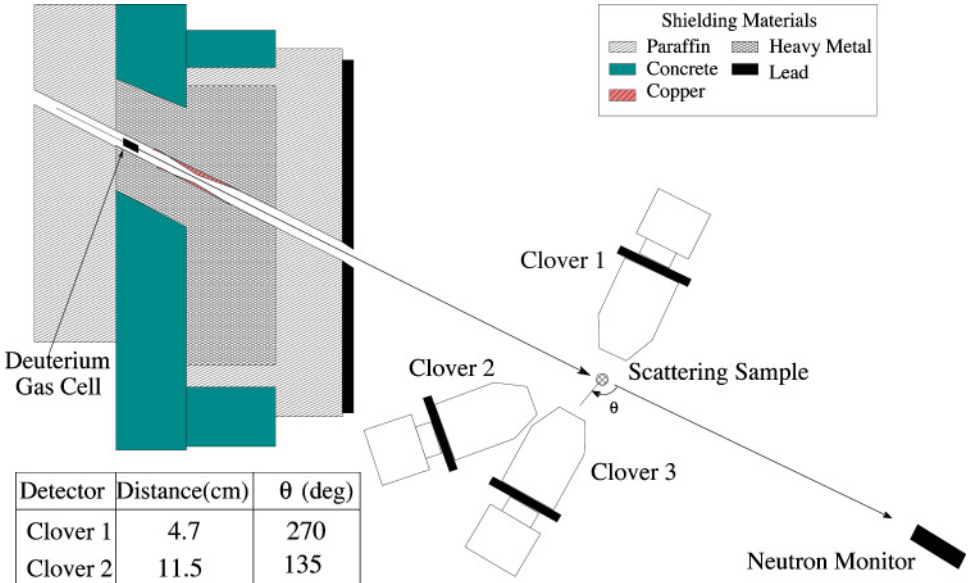

Detector	Distance(cm)	θ (deg)
Clover 1	4.7	270
Clover 2	11.5	135
Clover 3	5.8	118

FIG. 3. (Color online) A schematic diagram (not to scale) of the coincidence arrangement at the TUNL facility. The detector distances were measured from the scattering sample to the front window of the clover detectors, and the angles were measured with respect to the neutron beam in the clockwise direction.

The data acquisition for coincidences was performed with a scripted version of SpecTcl [27]. A two-dimensional matrix was built by a *.tcl* script in the SpecTcl environment and was analyzed off-line with TV spectral analysis software [28]. Because a continuous beam was used for these measurements, the firing time of quadrant 1 in clover 1 was used as a universal time reference for recording any event in all the other quadrants of the three clover detectors. The coincidence resolving time between any 2 clovers was set electronically to about 120 ns to record the coincident events. More stringent time constraints were applied when the E_γ-E_γ coincidence matrix was constructed off-line. An example of a coincidence spectrum, gated on the $2_1^+ \rightarrow 0_1^+$ transition, is shown in Fig. 4.

C. Data analysis

Energy thresholds for γ-ray emission and limitations on the spin of the level from which a transition arises are determined from the excitation function measurements, as described in Ref. [29]. The experimental cross sections of the excited states as a function of incident neutron energy provide information about the spins of the excited levels, when compared to the results from the statistical model given by a modified version of the code CINDY [30]. Along with the excitation function data, the coincidence data were used to place new γ-ray transitions and a level scheme was constructed.

The INS reaction at low incident neutron energies occurs mainly through the compound-nucleus mechanism [31]. The resulting anisotropic angular distributions of γ rays emitted from the excited levels due to the alignment of the excited nuclei provide information about the multipolarity of the transitions [32]. The spin of the level from which the γ ray has been emitted and the corresponding multipole mixing ratios, δ, were determined by comparison of the experimental yields of the γ rays to the theoretical calculations given by a modified version of the code CINDY [30], which is based on the statistical compound nucleus theory.

An example of the angular distribution data analysis is given in Fig. 5 for the 752.5-keV γ ray, the $2_2^+ \rightarrow 2_1^+$ transition, for which the two values of δ have similar χ^2 values in the χ^2 vs. δ plot. The δ value of 0.02(2) was selected for this transition, as the other δ gives an unrealistic $B(E2)$ value [24]. The $2 \rightarrow 2$ origin for this transition is supported by the χ^2 vs. δ plot. Also, from the ground-state transition of this level, i.e., the 1671.4-keV γ ray, $J_i^\pi = 2^+$ is confirmed. From these data, along with the branching ratios, BR, and lifetimes, τ, the reduced transition probabilities [$B(M1)$, $B(E2)$, etc.] were obtained.

Among the important properties deduced from the angular distribution measurements are the lifetimes of the excited levels. With the DSAM [33], lifetimes of the excited levels in the range of a few fs to about 1 ps are determined. Following inelastic neutron scattering the nucleus recoils and the γ rays produced experience an attenuated Doppler shift. If E_γ^0 is the energy of a γ ray emitted by the nucleus at rest, the energy of the Doppler-shifted γ ray as a function of the observation angle, $E_\gamma(\theta_\gamma)$, is expressed by:

$$E_\gamma(\theta_\gamma) = E_\gamma^0 \left[1 + \frac{v_{\text{c.m.}}}{c} F(\tau) \cos\theta_\gamma\right], \qquad (1)$$

where $v_{\text{c.m.}}$ is the initial velocity of the center-of-mass of the recoiling excited nucleus and the outgoing particle in the laboratory frame. $F(\tau)$ is the attenuation factor related to the stopping process described by Blaugrund [34], and its experimental value, $F_{\text{exp}}(\tau)$, is related to the slope of the E_γ vs. $\cos\theta_\gamma$ plot. It is then compared with the theoretical value calculated with the Winterbon formalism [35], and the lifetime, τ, is determined. The $\overline{F}(\tau)$ for a level, as listed in Table II, is the weighted average value of the $F_{\text{exp}}(\tau)$s of the γ ray from that level. An example of this analysis is shown in Fig. 6, for the 752.5-keV γ ray.

TABLE II. Observed levels and corresponding γ-ray transitions in ^{94}Zr. I_γ gives the relative intensities of the γ rays from a given level summed to 100. There is a 10% systematic uncertainty in the $\overline{F}(\tau)$ value due to uncertainty in the stopping process. For most of the transitions, the multipole mixing ratio, δ, with the minimum χ^2 is given. Both δ values are reported when they have similar values of χ^2. γ denotes a new transition, and L signifies a level established in this work. The spin assignments were obtained from the angular distribution, denoted by J (AD), or excitation function data, denoted by J(Exf). The J^π values in parentheses are tentativly assigned spins from this work. A known level, also observed with the INS reaction in this work, is marked as INS.

E_x (keV)	J_i^π	J_f^π	E_γ (keV)	I_γ (%)	$\overline{F}(\tau)$	τ (fs)	δ or λl	Notes
918.82(2)	2_1^+	0_1^+	918.82(2)	100	–	9.9(21) ps	$E2$	[a]
1300.39(2)	0_2^+	2_1^+	381.58(10)	100	–	420(16) ps	$E2$	[a]
1469.70(2)	4_1^+	2_1^+	550.78(10)	100	–	721(18) ps	$E2$	[a]
1671.45(2)	2_2^+	2_1^+	752.50(10)	42(1)	0.180(11)	183^{+13}_{-12}	0.02(2)	[b,c]
							2.2(5)	
		0_1^+	1671.40(10)	58(1)			$E2$	[b]
2057.87(2)	3_1^-	4_1^+	588.05(10)	2.5(5)	0.351(20)	73(6)	$E1$	
		2_1^+	1138.96(5)	97.5(5)			$E1$	
2151.34(2)	2_3^+	2_2^+	479.90(20)	5(1)	0.097(22)	337^{+100}_{-65}	$1.6^{+0.7}_{-0.6}$	γ [c]
							$0.19^{+0.25}_{-0.15}$	
		2_1^+	1232.40(10)	93(1)			$-0.75^{+0.04}_{-0.05}$	
		0_1^+	2151.30(30)	2(1)			$E2$	γ
2329.97(2)	4_2^+	2_2^+	658.45(5)	5.5(3)	0.127(14)	280^{+40}_{-33}	$E2$	γ
		2_1^+	1411.11(5)	94.5(3)			$E2$	
2366.34(2)	2_4^+	3_1^-	308.50(5)	8(1)	0.094(11)	387^{+60}_{-45}	$E1$	
		2_2^+	694.80(5)	40(1)			$2.90^{+0.35}_{-0.25}$	
							$-0.07^{+0.03}_{-0.04}$	
		0_2^+	1065.89(5)	10.5(5)			$E2$	
		2_1^+	1447.55(20)	41.5(5)			$0.65^{+0.25}_{-0.20}$	
2507.92(2)	3_1^+	2_3^+	356.6(5)	3(2)	0.070(14)	522^{+137}_{-90}		J (AD, Exf), γ [d]
		2_2^+	836.39(10)	14(2)			$-0.90^{+0.40}_{-0.45}$	
		2_1^+	1589.15(20)	83(2)			$1.50^{+0.25}_{-0.75}$	
2605.39(3)	5_1^-	4_1^+	1135.67(30)	100	0.201(41)	160^{+50}_{-33}	$E1$	
2698.45(3)	(1)	2_3^+	547.30(7)					J (AD), γ [d]
		2_1^+	1779.32(10)					[e]
		2_2^+	1026.91(20)					γ [f]
		0_1^+	2698.88(35)					γ
2826.75(3)	3_2^+	2_2^+	1155.27(2)	88.5(5)	0.209(25)	166^{+27}_{-22}	0.40(3)	J(Exf, AD)
		2_1^+	1907.91(4)	11.5(5)			$0.52^{+0.16}_{-0.12}$	γ
							$0.30^{+1.66}_{-0.24}$	
2846.36(3)	1^-	2_1^+	1927.30(10)	–	0.962(16)	$2.10^{+0.93}_{-0.90}$	$E1$	J (AD) [e]
		0_1^+	2846.36(5)	100(10)			$E1$	
2860.70(3)	(5^+)	4_1^+	1390.99(2)	100	0.138(24)	270^{+64}_{-45}	$0.35^{+0.05}_{-0.04}$	J(Exf, AD)
2873.65(3)	(4^+)	4_2^+	543.74(20)	27(1)	0.189(27)	187^{+37}_{-28}	$E2/M1$	L, J (AD, Exf), γ [d]
		4_1^+	1403.93(2)	60(1)			$E2/M1$	γ [d]
		2_1^+	1954.91(7)	13(1)			$E2$	γ
2888.25(7)	4^+	2_1^+	1969.42(5)	100	0.231(17)	145^{+14}_{-12}	$E2$	
2908.04(2)	2_5^+	2_3^+	756.71(3)	22.5(6)	0.211(17)	163^{+18}_{-15}	$-0.04^{+0.09}_{-0.08}$	INS, J (AD, Exf), γ
							$2.70^{+0.95}_{-0.60}$	
		2_2^+	1236.57(2)	45(1)			$E2/M1$	[d]
		2_1^+	1989.21(3)	17.5(7)			$0.73^{+0.60}_{-0.45}$	
		0_1^+	2908.05(10)	15(1)			$E2$	
2927.50(5)	3_2^-	4_1^+	1457.79(4)	100	0.141(56)	260^{+200}_{-85}	$E1$	γ, INS, J (AD)
2945.33(5)	5_2^-	3_1^-	887.46(3)	100	0.028(71)	>380	$E2$	J (AD)

TABLE II. (*Continued.*)

E_x (keV)	J_i^π	J_f^π	E_γ (keV)	I_γ (%)	$\overline{F}(\tau)$	τ (fs)	δ or λl	Notes
3000.01(4)	–	2_1^+	2081.27(3)	100	0.175(26)	202^{+40}_{-30}		L, γ, J(Exf)[d]
3029.72(13)	(5^+)	4_1^+	1560.01(10)	100	0.000(32)	>1250	$-0.28^{+0.08}_{-0.09}$	INS, J(Exf, AD), γ
3056.35(13)	(2^+)	2_1^+	2137.5(10)	100	0.304(68)	100^{+40}_{-25}	$1.6^{+0.5}_{-0.4}$	L, γ, J (AD)
							$0.15^{+0.15}_{-0.08}$	
3058.50(50)	$2^{(-)}$	2_2^+	1385.08(50)	45(1)	0.517(24)	43(4)	$-0.06(6)$	L, J (AD)
		2_1^+	2141.06(50)	55(1)			$-0.13(8)$	
3089.39(46)	(4^-)	3_1^-	1031.48(5)	55(1)	0.157(43)	228^{+100}_{-57}	$-0.32(8)$	L, J(Exf, AD), γ
		4_1^+	1619.7(5)	45(1)			$-0.14(12)$	γ
3141.66(4)	(4^+)	4_2^+	811.68(2)	100	0.265(45)	120^{+30}_{-25}	$-0.01^{+0.09}_{-0.08}$	L, J(Exf), γ
							$1.24^{+0.28}_{-0.24}$	
3155.93(3)	(4^+)	2_1^+	2237.11(2)	100	0.466(17)	51(3)	$E2$	
3200.28(4)	$1^{(+)}$	2_1^+	2281.73(11)	11.5(2)	0.838(47)	$9.4^{+3.3}_{-3.0}$	$E2/M1$	L, J(Exf), γ[d]
		0_1^+	3200.27(3)	88.5(2)			$M1$	γ
3219.72(4)	(3^+)	2_3^+	1069.58(50)	22.5(8)	0.321(29)	94^{+13}_{-11}	$2.05^{+0.75}_{-0.70}$	J (AD), γ
							$0.85^{+2.40}_{-0.22}$	
		3_1^-	1161.82(3)	52(1)			$E1$	
		4_1^+	1751.04(11)				$E2/M1$	[e]
		2_1^+	2301.44(10)	25.5(8)			$E2/M1$	[d]
3224.84(4)	(4^+)	4_1^+	1755.22(10)	75(1)	0.346(27)	82^{+10}_{-9}	$0.09^{+0.25}_{-0.14}$	L, J (AD), γ
							$0.99^{+0.38}_{-1.00}$	
		2_1^+	2305.98(10)	25(1)			$E2$	γ
3284.46(6)	(2^+)	3_1^-	1226.34(5)	34(1)	0.476(30)	49^{+6}_{-5}	$E1$	INS, γ
		2_1^+	2365.65(5)	58(2)			$1.95^{+0.70}_{-0.45}$	γ
		0_1^+	3284.29(16)	8(2)			$E2$	γ
3318.63(7)	2^+	2_2^+	1647.00(50)	51(5)	0.527(41)	40^{+7}_{-6}	$E2/M1$	INS, J (AD), γ[d]
		0_1^+	3318.63(5)	49(5)			$E2$	γ
3331.34(65)	(1^+)	2_1^+	2412.51(50)	100	0.134(87)	268^{+560}_{-120}	$E2/M1$	INS, J (AD), γ[d]
3336.22(65)	(5^+)	4_1^+	1866.52(50)	100	0.451(80)	53^{+20}_{-14}	0.5(1)	γ, INS, J (AD)
3361.41(6)	(3)	2_4^+	996.77(3)	–	0.355(42)	78^{+16}_{-12}		J(Exf), γ[f]
		4_1^+	1891.68(4)	74(2)				
		2_1^+	2442.86(14)	26(2)				[d]
3411.21(12)	(4^+)	2_1^+	2492.38(10)	100	0.774(78)	14^{+6}_{-5}	$E2$	INS, J(Exf), γ
3482.33(13)	(4^+)	4_1^+	2012.6(1)					INS, J(Exf), γ
3551.96(13)	–	2_1^+	2633.1(2)					INS, γ
3553.13(13)	(5^+)	4_1^+	2083.4(1)					L, J(Exf), γ
3561.93(26)	(5^+)	4_1^+	2092.2(2)					INS, J(Exf), γ
3579.56(13)	(4^+)	2_1^+	2660.7(1)					L, J(Exf), γ
3597.36(13)	(5^-)	2_1^+	2678.5(1)					INS, J(Exf), γ[g]
3699.23(13)	(4^+)	4_1^+	2229.5(1)					L, J(Exf), γ

[a]Lifetime value is from Ref. [21].
[b]The value for the branching ratio is different from Refs. [21] and [22].
[c]The lifetime values are slightly different from previously reported values in Ref. [24]. The source of this difference is explained in Ref. [41].
[d]No δ value could be obtained from the angular distribution, due to the small cross section of the transition.
[e]This transition was on a background peak and is not included in determining the branching ratios and lifetime.
[f]The placement of the transition is uncertain and is not included in determining the branching ratios and lifetime.
[g]Spin assignment from Ref. [21].

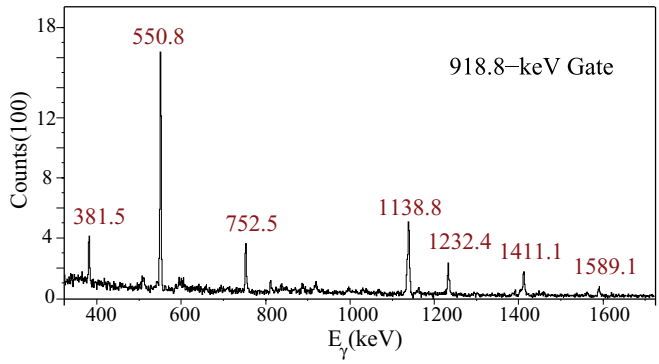

FIG. 4. (Color online) Coincidence spectrum gated on the 918.8-keV ($2_1^+ \rightarrow 0_1^+$) transition.

III. EXPERIMENTAL RESULTS AND LEVEL DISCUSSION

In the earlier INS measurements on ^{94}Zr by Glasgow and coworkers [23], a level scheme up to 3.361 MeV was established. Also, branching ratios and multipole mixing ratios for the transitions observed in the angular distribution measurements up to the 2887.7-keV level were reported. Without lifetimes, however, no transition strengths were obtained.

Our study of the low-lying states in ^{94}Zr with the INS reaction provides level-scheme information, including lifetimes and multipole mixing ratios, up to 3.4 MeV. A total of 38 new transitions and 8 new levels were established. The experimental information is listed in Table II, where L and γ denote a newly observed level or γ-ray transition. Also, 14 previously known excited states, as given in Ref. [21], were observed for the first time with the INS reaction; these levels are marked with INS. Lifetimes for 31 levels, and branching ratios and multipole mixing ratios for the corresponding γ rays, which were obtained from the angular distribution measurements at $E_n = 2.3$, 2.8, and 3.5 MeV, were used to obtain the reduced transition probabilities that are listed in Table III. For excited levels above the 3.411-MeV level, data from the excitation functions, performed up to $E_n = 4.0$ MeV, and $\gamma\gamma$ coincidences at $E_n = 5.0$ MeV were used to establish a level scheme up to $E_x = 3.7$ MeV. Those γ rays listed in Table IV could not be placed in the level scheme. E_n refers to the incident neutron energy of the excitation function at which the γ ray was first observed.

The experimental results indicate interesting and puzzling decay properties for the low-lying states in ^{94}Zr. Some of the levels are discussed in this section, and other interesting results are discussed in greater detail in Sec. IV.

A. 2_2^+ state at 1671.4 keV

The spin and parity of this state were determined previously [21] and were confirmed from our data. A lifetime of $\tau = 183^{+13}_{-12}$ fs was determined from the DSAM measurements at $E_n = 2.3$ MeV. The branching ratios for the two γ rays depopulating this level were also measured from the same data and are in disagreement with the NDS database [21]. Our results are, however, in agreement with the ^{94}Y β^- decay results, where intensities of $I_\gamma(752.6\,\text{keV}) = 2.5(2)$ and $I_\gamma(1671.4\,\text{keV}) = 4.4(4)$ were measured.

In the INS measurements on ^{94}Zr by Glasgow *et al.* [23], the branching ratios of the γ rays depopulating a level were determined from the γ-ray cross sections, $\sigma_\gamma(E_\gamma)$ (mb). These values were obtained from the a_2 and a_4 expansion coefficients in a least-squares polynomial fit to the angular distribution data at $E_n = 3.1$ MeV and are given in Table IV of Ref. [23]. The data showed a σ_γ of 169(16) for the 752.3-keV γ ray and 247(24) for 1671.8-keV γ ray, which naturally would result in a higher I_γ (and branching ratio) for the 1671.8-keV transition. Unfortunately, the NDS compiled data in the ^{94}Zr level scheme of Fig. 21 of Ref. [23], shows 59 and 41 as branching ratios for 752.3- and 1671.8-keV transitions, respectively. These values appear to have been inverted in the NDS [21] and NNDC data for ^{94}Zr [22].

The stronger decay branch to the ground state, the 1671.4-keV transition, gives a $B(E2)$ value of 7.8(7) W.u. This is the only known case in which the $B(E2; 2_2^+ \rightarrow 0_1^+)$ is larger than the $B(E2; 2_1^+ \rightarrow 0_1^+)$. The multipole mixing ratio for the 752.5-keV transition, $\delta = 0.02(2)$, shown in Fig. 5 results in $B(M1) = 0.31(3)\ \mu_N^2$. This state has been identified as the one-phonon MS state, with an anomalous decay behavior [24], and is discussed in greater detail in Sec. IV.

B. 2_3^+ state at 2151.3 keV

In addition to the known $2_3^+ \rightarrow 2_1^+$ 1232.4-keV transition, new transitions to the 2_2^+ state, $E_\gamma = 479.9$ keV, and the ground state were observed in this work. This state has been identified as a two-phonon symmetric excitation [24].

A careful analysis of the angular distribution of the $2_3^+ \rightarrow 2_2^+$ 479.9-keV γ ray resulted in δ values of $1.6^{+0.7}_{-0.6}$ and $0.19^{+0.25}_{-0.15}$, which have similar χ^2 values. The resulting

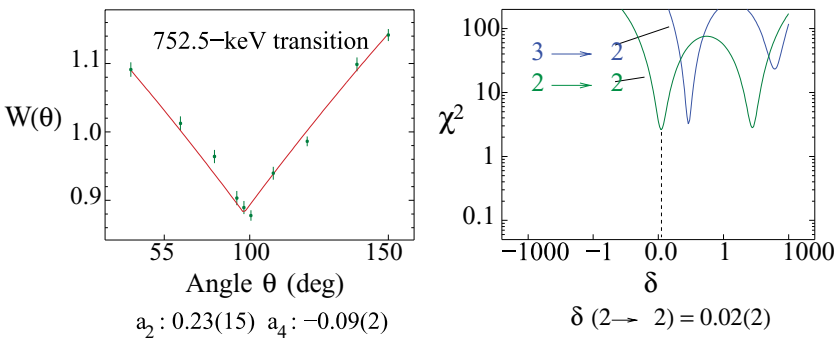

FIG. 5. (Color online) Angular distribution data for the 752-keV γ ray, with a polynomial least-squared fit to the data. Note that the scale is linear in $\cos^2\theta$. The spin assignment and δ determination based on comparison of the data to the theoretical calculations is confirmed from the χ^2 vs. δ plot [24].

TABLE III. The reduced transition probabilities, $B(\lambda l)\downarrow$, calculated for the γ-ray transitions between low-lying states in ^{94}Zr. The $B(E1)\downarrow$ values are given in mW.u. ($= 1.33 \times 10^{-3}\ e^2\ \mathrm{fm}^2$ for ^{94}Zr). The $B(M1)\downarrow$ and $B(E2)\downarrow$ values are given in μ_N^2 and W.u., respectively. For $B(E2)$ values, 1 W.u. $= 25.387\ e^2\ \mathrm{fm}^4$ for ^{94}Zr.

E_x (keV)	J_i^π	J_f^π	E_γ (keV)	Notes	$B(E1)\downarrow$ (mW.u.)	$B(M1)\downarrow$ (μ_N^2)	$B(E2)\downarrow$ (W.u.)
918.82(2)	2_1^+	0_1^+	918.82(2)	[a]			4.9(3)
1300.39(2)	0_2^+	2_1^+	381.58(10)	[a]			9.4(4)
1469.70(2)	4_1^+	2_1^+	550.78(10)	[a]			0.878(23)
1671.45(2)	2_2^+	2_1^+	752.50(10)			0.31(3)	$0.12^{+0.25}_{-0.12}$
							250(50)
		0_1^+	1671.40(10)				7.8(7)
2057.87(2)	3_1^-	4_1^+	588.05(10)		0.8(2)		
		2_1^+	1138.96(5)		$4.3^{+0.4}_{-0.3}$		
2151.34(2)	2_3^+	2_2^+	479.90(20)			$0.07^{+0.04}_{-0.03}$	7^{+4}_{-3}
						$0.012^{+0.009}_{-0.007}$	135^{+115}_{-75}
		2_1^+	1232.40(10)			$0.05^{+0.02}_{-0.01}$	11(3)
		0_1^+	2151.30(30)				$0.04^{+0.04}_{-0.02}$
2329.97(2)	4_2^+	2_2^+	658.45(5)				52^{+10}_{-8}
		2_1^+	1411.11(5)				19^{+3}_{-2}
2366.34(2)	2_4^+	3_1^-	308.50(5)		3.3(5)		
		2_2^+	694.80(5)			$0.18^{+0.03}_{-0.02}$	1.02(15)
						0.018(5)	187^{+55}_{-40}
		0_2^+	1065.89(5)				6(1)
		2_1^+	1447.55(20)			0.014(3)	$1.6^{+0.5}_{-0.4}$
2507.92(2)	3_1^+	2_3^+	356.6(5)	[b]			
		2_2^+	836.39(10)			$0.014\ ^{+0.008}_{-0.006}$	10(5)
		2_1^+	1589.15(20)			$0.006\ ^{+0.005}_{-0.002}$	4^{+1}_{-2}
2605.39(3)	5_1^-	4_1^+	1135.67(30)		$2.0^{+0.6}_{-0.5}$		
2698.45(3)	(1)	2_3^+	547.30(7)	[b,d]			
		2_1^+	1779.32(10)	[c]			
		2_2^+	1026.91(20)	[b]			
		0_1^+	2698.88(35)				
2826.75(3)	3_2^+	2_2^+	1155.27(2)			0.17(3)	11.5(2)
		2_1^+	1907.91(4)			0.004(1)	$0.18\ ^{+0.05}_{-0.04}$
						$0.0005^{+0.0003}_{-0.0004}$	$0.8^{+0.8}_{-0.4}$
2846.36(3)	1^-	2_1^+	1927.30(10)	[c]			
		0_1^+	2846.36(5)		10^{+7}_{-3}		
2860.70(3)	(5^+)	4_1^+	1390.99(2)			0.07(2)	$2.5^{+0.6}_{-0.5}$
2873.65(3)	(4^+)	4_2^+	543.74(20)	[b]			
		4_1^+	1403.93(2)	[b]			
		2_1^+	1954.91(7)				0.8(2)
2888.25(7)	4^+	2_1^+	1969.42(5)				7.5(7)
2908.04(2)	2_5^+	2_3^+	756.71(3)			0.18(2)	$0.3^{+1.0}_{-0.3}$
						$0.017^{+0.007}_{-0.008}$	130^{+74}_{-48}
		2_2^+	1236.57(2)	[b]			
		2_1^+	1989.21(3)			0.005(2)	$0.4^{+0.2}_{-0.1}$
		0_1^+	2908.05(10)				0.14(3)
2927.50(5)	3_2^-	4_1^+	1457.79(4)		0.6(3)		
2945.33(5)	5_2^-	3_1^-	887.46(3)				<150
3000.01(4)	–	2_1^+	2081.27(3)	[b]			
3029.72(13)	(5^+)	4_1^+	1560.01(10)			<0.01	<0.20
3056.4(5)	(2^+)	2_1^+	2137.5(1)			0.02(1)	5(2)
						0.06(2)	$0.16^{+0.06}_{-0.05}$

TABLE III. (*Continued.*)

E_x (keV)	J_i^π	J_f^π	E_γ (keV)	Notes	$B(E1)\downarrow$ (mW.u.)	$B(M1)\downarrow$ (μ_N^2)	$B(E2)\downarrow$ (W.u.)
3058.50(50)	$2^{(-)}$	2_2^+	1385.08(50)		$1.89^{+0.19}_{-0.16}$		
		2_1^+	2141.06(50)		$0.62^{+0.06}_{-0.05}$		
3089.39(46)	(4^-)	3_1^-	1031.48(5)			0.11(4)	5(2)
		4_1^+	1619.7(5)		0.22(8)		
3141.66(4)	(4^+)	4_2^+	811.68(2)			$0.89^{+0.22}_{-0.20}$	$0.08^{+1.24}_{-0.08}$
						$0.28^{+0.11}_{-0.09}$	375^{+160}_{-120}
		2_2^+	1470.0(5)	[b,c]			
3155.93(3)	(4^+)	2_1^+	2237.11(2)				11(1)
3200.28(4)	$1^{(+)}$	2_1^+	2281.73(11)	[c]			
		0_1^+	3200.27(3)			$0.16^{+0.08}_{-0.04}$	
3219.72(4)	(3^+)	2_3^+	1069.58(50)			0.02(1)	46^{+28}_{-22}
						$0.05^{+0.02}_{-0.05}$	18^{+36}_{-5}
		3_1^-	1161.82(3)		1.7(2)		
		4_1^+	1751.04(11)	[c]			
		2_1^+	2301.44(10)	[c]			
3224.84(4)	(4^+)	4_1^+	1755.22(10)			$0.095^{+0.015}_{-0.014}$	$0.14^{+0.72}_{-0.14}$
						$0.05^{+0.05}_{-0.02}$	9^{+3}_{-9}
		2_1^+	2305.98(10)				$1.5^{+0.2}_{-0.2}$
3284.46(6)	(2^+)	3_1^-	1226.3(5)		1.8(3)		
		2_1^+	2365.65(5)			0.014(6)	4^{+2}_{-1}
		0_1^+	3284.29(16)				$0.14^{+0.05}_{-0.04}$
3318.63(7)	2^+	2_2^+	1647.00(50)	[c]			
		0_1^+	3318.63(5)				$0.98^{+0.29}_{-0.23}$
3331.34(65)	(1^+)	2_1^+	2412.51(50)	[c]			
3336.22(65)	(5^+)	4_1^+	1866.52(50)			$0.13^{+0.06}_{-0.04}$	5(2)
3361.41(6)	(3)	2_4^+	996.77(3)	[c]			
		4_1^+	1891.68(4)				
		2_1^+	2442.86(14)				
3411.21(12)	(4^+)	2_1^+	2492.38(10)				24^{+14}_{-7}

[a]From Ref. [21].
[b]No δ value could be obtained from the angular distribution.
[c]The parity of the state was not determined; therefore, no transition strengths were provided.
[d]The γ-ray peak was near a background peak.

TABLE IV. γ rays observed in the ^{94}Zr$(n,n'\gamma)$ spectrum, which could not be placed in the level scheme. E_n gives the lowest neutron energy at which the γ ray is first observed.

E_γ(keV)	E_n(MeV)
1398.1(1)	2.8
1484.3(1)	3.5
1855.6(1)	3.4
1981.4(1)	2.9
2252.8(2)	3.6
2398.5(1)	3.5
2561.9(1)	3.7
2671.3(2)	3.7
3156.3(1)	3.5
3547.6(2)	3.7
3660.8(2)	3.9
3681.3(2)	3.9
3871.6(2)	3.9

transition strengths for the larger δ are $B(E2) = 135^{+115}_{-75}$ W.u. and $B(M1) = 0.012^{+0.009}_{-0.007}\ \mu_N^2$. If this $B(E2)$ value is considered to be nonphysical, then the corresponding δ value should be discarded. The latter value, however, results in a non-negligible $B(M1)$ value of $0.07^{+0.04}_{-0.03}\ \mu_N^2$ for this transition and $B(E2) = 7^{+4}_{-3}$ W.u. Also, even though the 1232.4-keV γ ray, the $2_3^+ \rightarrow 2_1^+$ transition, is dominantly $E2$, its $B(M1)$ is $0.05^{+0.02}_{-0.01}\ \mu_N^2$, which is larger than the limit of 0.01 μ_N^2 for transitions between symmetric multiphonon states with $\Delta N_{\text{phonon}} = 1$ [19]. It will be noted that the $B(M1)$ values in ^{94}Zr do not fit within that limit, and the level scheme does not fall into the description of the nearly spherical nuclei given by the Q-phonon scheme, as described in Ref. [19].

C. 4_2^+ state at 2329.9 keV

With a lifetime of 280^{+40}_{-33} fs, this level decays predominantly to the 2_1^+ state. A new $4_2^+ \rightarrow 2_2^+$ transition was also observed,

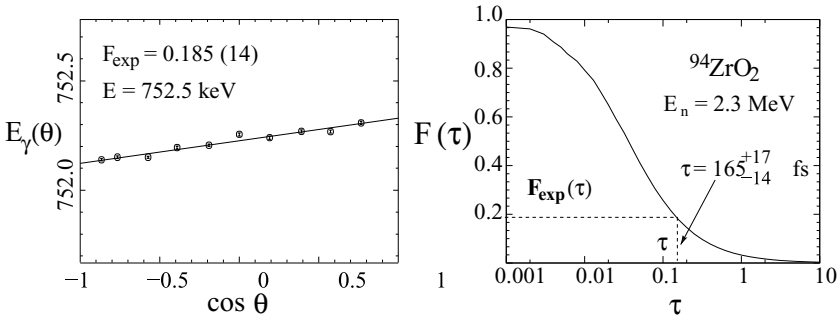

FIG. 6. Experimental E_γ vs. cos θ plot, for the 752.5-keV γ ray and the lifetime deduced from the theoretical $F(\tau)$ plot. The weighted average lifetime of the 1671.4-keV level from which the 752.5-keV γ ray arises is 183^{+13}_{-12} fs. Data are from the ^{94}Zr$(n, n'\gamma)$ angular distribution at $E_n = 2.3$ MeV.

which with a small branching ratio, 5.5(3)%, results in a large $B(E2) = 52^{+10}_{-8}$ W.u. The decay branch to the 4^+_1 state reported in NDS [21] was not observed in this work. It is surprising that the $E2$ decay branch from the 4^+_2 state to the 2^+_1 state is much stronger than the $4^+_1 \rightarrow 2^+_1$ transition, $B(E2; 4^+_1 \rightarrow 2^+_1) = 0.878(23)$ W.u. [21]. The negative g factor, $-0.8(4)$, measured for the 4^+_1 state [36] indicates a dominant neutron contribution to the wave function. No additional information is available for the 4^+_2 state.

D. 2^+_4 state at 2366.3 keV

All the known transitions [21] have been observed in this work. The δ values for these transitions are in agreement with the results of Glasgow *et al.* [23], although different signs resulted from that work, where the Rose and Brink phase convention was used [37].

Two δ values were possible for the $2^+_4 \rightarrow 2^+_2$694.8-keV transition, $\delta_1 = 2.90^{+0.35}_{-0.25}$ and $\delta_2 = -0.07^{+0.03}_{-0.04}$. In this case, similar to the aforementioned 479.9-keV transition from the 2151.3-keV level, δ_1 results in a very large $B(E2)$ value of 187^{+55}_{-40} W.u., whereas δ_2 results in a much smaller $B(E2)$ value, but a relatively large $B(M1)$ value of $0.18^{+0.03}_{-0.02}$ μ^2_N. The similarity between this transition and the 479.9-keV, $2^+_3 \rightarrow 2^+_2$ transition, could be attributed to the characteristics of the 2^+_2 state, which has been identified as an anomalous one-phonon MS state [24]; both transitions populate the 2^+_2 state.

E. 3^+_1 state at 2507.9 keV

The spin was assigned to this level from both the angular distribution and excitation function data. In addition to the known transitions to the 2^+_2 and 2^+_1 states, a new weak transition to the 2^+_3 state was observed in this work, but the angular distribution data were insufficient to provide a value for the mixing ratio of this transition. For the $3^+_1 \rightarrow 2^+_2 E2$ transition, $B(E2) = 10(5)$ W.u. is larger than that for the $3^+_1 \rightarrow 2^+_1$ transition, $B(E2) = 4^{+1}_{-2}$ W.u.

F. (1) state at 2698.4 keV

The 1779.3-keV transition to the 2^+_1 state has been observed in our singles and $\gamma\gamma$ coincidence spectra. However, it could not be included in the angular distribution and DSAM data analysis, as this γ ray is at the same energy as a γ ray in ^{28}Si, a background radiation (see Fig. 2). New transitions to the 2^+_3, 2^+_2, and 0^+_1 states were observed, and their excitation functions showed the same threshold. Because these transitions were relatively weak, no δ values could be determined from their nearly isotropic angular distributions. However, from the excitation function and the angular distribution of the ground-state transition, the spin assignment was limited to (1), from (1, 2, 3) given in Ref. [21]. The lifetime of the level deduced, without including the 1779.3-keV γ ray in the analysis, was $\tau = 102^{+56}_{-31}$ fs. Because the information on the branching ratios is problematic, no further analysis could be done.

G. 3^+_2 state at 2826.7 keV

In addition to a dominant transition to the 2^+_2 state, a decay branch to the 2^+_1 state was observed. The spin of this level is given in Ref. [21] as (2, 3). From the angular distributions, spin 3^+ was assigned and confirmed from the excitation function data. Again, the transition to the 2^+_2 state has a large $B(E2) =$ 11.5(2) W.u., accompanied by a relatively large $B(M1)$ value of 0.17(3) μ^2_N.

H. 1^- state at 2846.4 keV

For this state, the spin and parity (1^-) as given in Ref. [21] were confirmed from our excitation function and angular distribution data. The decay to the ground state is a fast $E1$ transition with $\tau = 2.10^{+0.93}_{-0.90}$ fs. This state was excited in the NRF measurements on ^{92}Zr, in which the scattering sample has had a contamination of 2.03% ^{94}Zr [38], confirming the $J = 1$ assignment. Also, unpublished NRF measurements on ^{94}Zr [39] agree with this spin assignment. A weak 1927.3-keV γ-ray transition to the 2^+_1 state was also observed. It could not be included in the angular distribution and DSAM data analysis, as there is a background γ-ray peak at the same energy from ^{63}Cu (see Fig. 2). Therefore, a branching ratio of 100(10) has been assigned for the stronger ground-state transition.

I. (5^+) state at 2860.7 keV

A spin and parity assignment of 4^+ is given in Ref. [21]. In the ^{94}Zr(d, d') experiments, spin 4 was assigned to a level at 2.87 MeV [40]. From our data, a tentative spin of (5^+) was assigned from the angular distribution data. A unique δ value

for a $5 \rightarrow 4$ transition was deduced from the χ^2 vs. δ plot. Also, the excitation function data favors $J^\pi = 5^+$. The only transition depopulating this level, $(5^+) \rightarrow 4_1^+$, has a relatively small $B(E2)$, $2.5^{+0.6}_{-0.5}$ W.u., and a non-negligible $B(M1)$ of 0.07(2) μ_N^2.

J. 2_5^+ state at 2908.0 keV

This level has been observed for the first time with the INS reaction. The assigned spin and parity, obtained from the angular distribution and excitation function data, confirm the results given in Ref. [21]. In addition to the known transitions to the 2_2^+, 2_1^+, and 0_1^+ states, a new transition to the 2_3^+ state has been observed, which has a $B(M1)$ value of 0.18(2) μ_N^2 and $B(E2) = 0.34(5)$ W.u. The 1236.5-keV transition to the 2_2^+ state, with 45(1)% branching ratio, has an anisotropic angular distribution with large uncertainties, from which no δ value could be deduced. If a pure $E2$ transition is assumed, the $B(E2)$ value is large, 30(3) W.u. (shown with dashed arrow in Fig. 7). Therefore, if the 2_3^+ state is considered as the two-phonon symmetric state, then the large $B(M1)$ of the $2_5^+ \rightarrow 2_3^+$ transition and the large $B(E2)$ of the $2_5^+ \rightarrow 2_2^+$ transition indicate that the 2_5^+ state is a good candidate for the 2^+ two-phonon MS state, $2^+_{2,\mathrm{ms}}$, in the multiphonon scheme. The energy of this state, 2908.0 keV, is close to the sum energy of the 2_2^+ and 0_2^+ states, which supports the candidacy of the 2_5^+ state as the 2^+ two-phonon MS state. The decay behavior of this state will be discussed in greater detail in Sec. IV.

K. $2^{(-)}$ state at 3058.5 keV

This newly observed state is different from the state at 3059.31(17) keV, given in Ref. [21] with $J^\pi = (1, 2, 3)^+$,

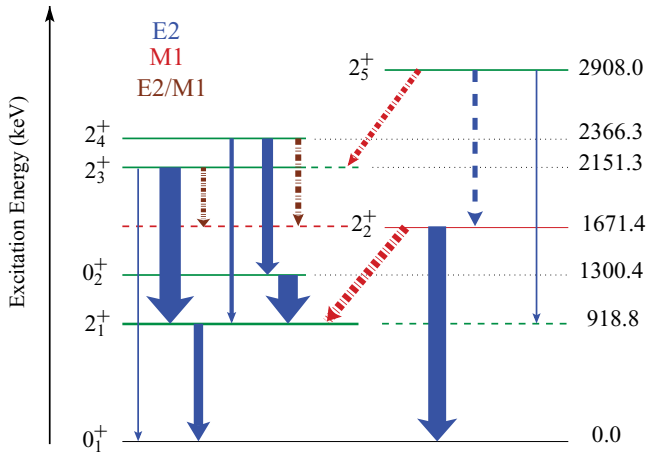

FIG. 7. (Color online) Comparison between the transitions to the 2_1^+ and 2_2^+ states. The widths of the arrows are proportional to the transition strengths, as listed in Table III. The solid-line (blue) arrows denote $E2$ transitions, whereas the dash-dotted (red) arrows indicate $M1$ transitions. Dash-double-dotted (brown) arrows are used for the transitions to the 2_2^+ state with large $E2$ and $M1$ transition rates. The dashed arrow for the $2_5^+ \rightarrow 2_2^+$ transition represents the $B(E2)$ value, if a pure $E2$ is considered; the angular distribution of this γ ray did not yield a unique δ value.

from which transitions were assigned at 1001.8(3), 1384.9(10), and 2140.60(20) keV, decaying to the 3_1^-, 2_2^+, and 2_1^+ states, respectively. In this work, the only transitions observed and confirmed from the $\gamma\gamma$ coincidences were the 1385.1- and 2141.1-keV γ rays, which are from a level at 3058.5 keV. A 1001-keV γ ray was observed in the angular distribution data, but the spectral peak could not be fitted and it was not included in the data. The lifetime of the level, $\tau = 43(4)$ fs, was obtained from the DSAM data, and for both transitions, two δ values were obtained. From the angular distribution data $J = 2$ was assigned.

The angular distribution of the 1385.1-keV γ ray yields $a_2 = 0.16(6)$ and $a_4 = -0.06(8)$, which indicates a large dipole component. Depending on the parity of the state, it could be an $M1$ or an $E1$ transition. One of the δ values for the $(2) \rightarrow 2_2^+$ transition is almost zero, $-0.06(6)$, indicating this transition could be $E1$. The same is true for the 2141.1-keV γ ray, $a_2 = 0.11(7)$ and $a_4 = -0.06(9)$, with one $\delta = -0.13(8)$ approaching zero. The energy of this level is very close to the sum energies of the 2_1^+ and 3_1^- states, making it a good candidate for a member of the $2_1^+ \otimes 3_1^-$ quintuplet. The $B(E1)$ value is $1.86^{+0.19}_{-0.16}$ mW.u. for the 1385.1-keV γ ray, and it is $0.62^{+0.06}_{-0.05}$ mW.u. for the 2141-keV transition.

L. (4^-) state at 3089.4 keV

The spin of this new level was assigned from the excitation function and the angular distribution of the 1031.5-keV γ ray, the stronger decay branch to the 3_1^- state, which favors $J = 4$, and it indicates a dominant dipole component; $a_2 = -0.72(12)$ and $a_4 = 0.09(15)$. From the nonzero δ value of $-0.32(8)$, this transition has mixed multipolarity, $E2/M1$ or $M2/E1$, depending of the parity of the initial state. A mixed $M2/E1$ transition is less likely; therefore, negative parity could be assigned to this state. The angular distribution of the 1619.7-keV γ ray, the decay to the 4_1^+ state, also indicates dipole character with $\delta = -0.14(12)$ for a $4 \rightarrow 4_1^+$ transition and supports the negative-parity assignment. Therefore, this level, along with (2^-) level at 3058 keV, could belong to the $2_1^+ \otimes 3_1^-$ quintuplet, because they fit the energy criteria.

M. (4^+) state at 3141.7 keV

In Ref. [21], a state at 3142.4(4) keV is given with $J^\pi = (6^+)$, which was observed in the high-spin studies of ^{94}Zr with the ^{173}Yb(^{24}Mg, $F\gamma$) and ^{176}Yb(^{28}Si, $F\gamma$) reactions [21,42], from the ground-state cascade of $6^+ \rightarrow 4^+ \rightarrow 2^+ \rightarrow 0^+$, comparisons to the neighboring isotopes, and shell-model predictions. Three transitions are listed from this state in Ref. [21], but only one transition similar in energy to the $J_i \rightarrow 4_2^+$, 812.5-keV transition has been observed in our work. Also, the previous spin assignment does not agree with our results.

The observed γ ray is at 811.68(2) keV, with a relatively large yield in the excitation function, which favors $J = 4$ and rules out a higher spin. Also, from the determined lifetime, $\tau = 120^{+30}_{-25}$ fs, an assumed $(6^+) \rightarrow 4_2^+$ pure $E2$

multipolarity for the 811.7-keV transition would lead to a $B(E2) = 620^{+140}_{-120}$ W.u., which is unrealistic.

A very weak branch to the 2^+_2 state, 1470.10(50) keV, has also been observed in the excitation function spectra and has the same threshold as the 811.7-keV transition. The angular distribution could not provide any additional information. Even though the peak at 1470.1 keV was not observed in the background spectra, it could be contaminated by the 1471.7-keV prompt γ ray in ^{74}Ge. This γ ray has not been included in our results, because the placement of this transition could not be confirmed from the $\gamma\gamma$ coincidence data.

Our results indicate that the level at 3141.7 keV is a newly observed level. A tentative spin (4^+) is assigned from the angular distribution data. The data in Table III shows this transition has a large $B(M1) = 0.89^{+0.22}_{-0.20}\ \mu_N^2$.

N. 4^+ state at 3155.9 keV

The spin and parity obtained from the angular distribution of the only γ-ray transition to the 2^+_1 state and the excitation function are in agreement with the (4^+) assignment given in Ref. [21]. This transition has $B(E2) = 11(1)$ W.u., which is reasonably large. The weak branch decay to the 3^+_1 state was observed in the excitation function spectra, but the peak could not be fitted and it was not included for determining branching ratios and lifetimes in Table II.

O. $1^{(+)}$ state at 3200.3 keV

This new level has a short lifetime, $\tau = 9.4^{+3.3}_{-3.0}$ fs, and decays predominantly to the ground state. A weaker branch decays to the 2^+_1 state. The spin (1^+) assignment was obtained from angular distribution and excitation function data. This state was first observed in the NRF measurements [39] and $J = 1$ has been assigned. The angular distribution of the 2281.7-keV transition provides no information on δ values. The ground-state transition has $B(M1) = 0.16^{+0.08}_{-0.04}\ \mu_N^2$, which is large and could make it a candidate for the two-phonon 1^+ MS state.

P. (3^+) state at 3219.7 keV

Spin (1,2,3) was assigned to this level in Ref. [21]. In addition to the known transitions to the 3^-_1 and 2^+_1 states, a new transition to the 2^+_3 state was observed. The transition to the 4^+_1 state, 1751.0 keV, was observed, but it is contaminated with a background γ ray. The spin of the level is limited to (2,3), because for spin 1, a transition to the 4^+_1 state would require $\Delta J = 3$, which is unlikely. The tentative spin (3) was assigned from the angular distribution. From the δ value of the $3 \rightarrow 3^-_1$ transition, $\delta = -0.064(64)$, which is small, this transition could be either $M1$ or $E1$. The transition to the 2^+ state has a nonzero δ value, which means it is not likely be a parity-changing transition, resulting in a positive parity assignment for this level.

Q. (4^+) state at 3411.2 keV

A level at 3407(6) keV, with spin $(3^-, 4^+)$, is given in Ref. [21] and was observed in the (d, d') and (α, α') reactions. The only transition, to the 2^+_1 state, has an isotropic angular distribution. A tentative spin (4^+) was obtained from the excitation function data. With this spin assignment, a pure $E2$ transition yields to $B(E2) = 24^{+14}_{-7}$ W.u.

IV. DISCUSSION

A. ^{94}Zr and collectivity

1. *Quadrupole-phonon excitations*

From the low-lying level scheme, as presented in Tables II and III, it is clear that ^{94}Zr does not fall into a simple vibrational picture. The 2^+_2 state at 1671.4 keV has a larger $E2$ ground-state transition, $B(E2) = 7.8(7)$ W.u., than the 2^+_1 state at 918.8 keV. Also, the $B(E2)$ value for the $2^+_1 \rightarrow 0^+_1$ transition, 4.9(3) W.u. [21], does not indicate significant collectivity and is smaller than that of ^{92}Zr.

Even if the 2^+_1 state is considered as the one-phonon symmetric state and the $E2$ transition, $B(E2; 0^+_2 \rightarrow 2^+_1) = 9.4(4)$ W.u. [21], suggests that the 0^+_2 state, at 1300 keV, belongs to the two-phonon triplet, but the energy is much lower than expected. However, the 2^+_3 state at 2151.3-keV decays with a dominant $E2$ transition to the 2^+_1 state, 11(2) W.u., and the energy of the level agrees with its assignment as a member of the two-phonon symmetric triplet. But this level also decays to the 2^+_2 state via a 479.9-keV γ ray, for which two δ values were obtained. One δ value results in an unrealistically large $B(E2)$, and the other δ in a smaller $B(E2)$, accompanied by a non-negligible $B(M1)$ value. There is no clear candidate for the third member of the two-phonon triplet, the 4^+ state. The $B(E2)$ of the transition from the 4^+_1 state at 1469.7 keV to the 2^+_1 state, 0.878(23) W.u. [21] is too small to indicate a collective excitation. The 4^+_2 state at 2329.9 keV has a larger $E2$ transition strength to the 2^+_1 state than that of the $4^+_1 \rightarrow 2^+_1$ transition, but the $E2$ transition to the 2^+_2 state is even larger than that of the $4^+_2 \rightarrow 2^+_1$ transition. More realistic assignments for these states have yet to be given. In general, the $B(E2)$ values or the energies of the aforementioned levels do not support a quadrupole vibrational structure in ^{94}Zr.

Transitions with large $B(M1)$ values are observed in ^{94}Zr. For example, the 2^+_5 state decays to the 2^+_3 state with a $B(M1) = 0.18(2)\ \mu_N^2$, but no δ value could be obtained from the angular distribution of the $2^+_5 \rightarrow 2^+_2$ transition. The $1^{(+)}$ level at 3200 keV, decays to the ground state, with a $B(M1)$ value of $0.18^{+0.08}_{-0.04}\ \mu_N^2$. A new (4^+) level at 3141 keV decays to the 4^+_2 state with a very large $B(M1)$ value, $0.89^{+0.24}_{-0.20}\ \mu_N^2$, even larger than the $B(M1; 2^+_2 \rightarrow 2^+_1)$ value (see Table III). Although large $B(M1)$ values are usually associated with MS states, these assignments could not be verified, as not all of the experimental signatures for MS states were observed.

Conclusively, there is no experimental evidence for quadrupole multiphonon excitations in ^{94}Zr; therefore, the low-lying excited states up to 3.15 MeV are classified according to their decay behavior. In particular, there are distinct differences between the states populating the 2^+_1 state and those decaying to the 2^+_2 state. The excited states with dominant $E2$ transitions to the 2^+_1 or the 2^+_2 state can be

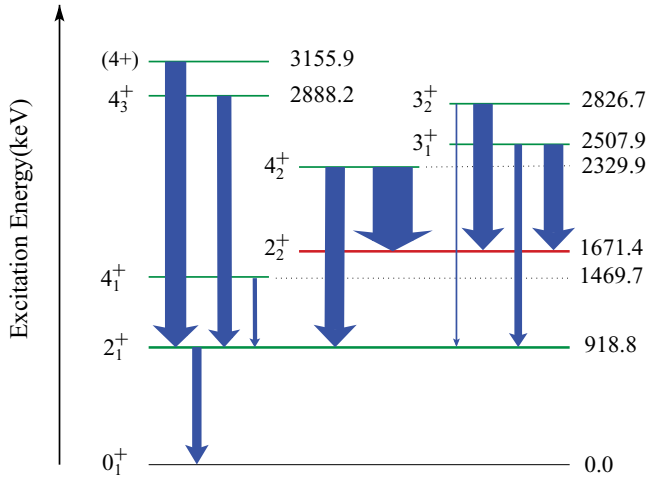

FIG. 8. (Color online) Comparison between the transitions from the 4^+ and 3^+ states to the 2_1^+ and 2_2^+ states. The widths of the arrows(blue) are proportional to the $E2$ transition strengths, as listed in Table III.

considered as excitations built on that respective state. Partial decay schemes of the positive-parity states depicting such behaviors are shown in Figs. 7 and 8 for transitions from the $J^\pi = 2^+$ and $J^\pi = 3^+, 4^+$ states, respectively. There are also several states which populate the 2_2^+ state via either pure $E2$ transitions, with unrealistic $B(E2)$ values, or smaller $B(E2)$s accompanied by a large $B(M1)$ value. Only the transitions from the 2_3^+ and 2_4^+ states, dashed-double-dotted arrows, are shown in Fig. 7. These are transitions for which a unique δ value could not be determined from the angular distribution data.

2. $2_1^+ \otimes 3_1^-$ *quintuplet*

Even though there is no experimental basis for the quadrupole multiphonon excitations, there are candidates for the $(2_1^+ \otimes 3_1^-)$ excitations. The energies of the 1^- state at 2846.4 keV, 3_2^- at 2927.5 keV, 5_2^- at 2945.3 keV, $2^{(-)}$ at 3058.5 keV, and (4^-) at 3089.4 keV are close to the summed energy of the 2_1^+ and 3_1^- states, which are 918.8 and 2057.9 keV, respectively. Even though these states fit the energy criteria, not all of them decay to the 2_1^+ or 3_1^- states, as expected, and the lower multipolarity $E1$ transitions dominate [43]. For example, the 3_2^- state only decays to the 4_1^+ state. The $B(E1)$ values observed are larger than the expected values in this region [44].

B. Comparison to other Zr isotopes

In ^{94}Zr, the valence neutrons and protons occupy the $\nu(d_{5/2})$ and $\pi(p_{1/2})$ shells, respectively. There is evidence of a subshell closure at $Z = 40$ in the Zr isotopes [3,45,46]. Therefore, one possibility for the choice of a core nucleus is ^{90}Zr, for proton excitation, core polarization, and excitations out of the subclosed shell are required, but many shell-model calculations have considered $^{88}_{38}$Sr as the core [45–47].

Even though $Z = 40$ is not a rigid subshell, there is evidence of its effect on the Zr isotopes. In a neutron-proton weak-coupling scheme, the experimental ^{92}Zr and ^{94}Zr level schemes were described in a calculation by Holt and coworkers [46], where realistic effective interactions were applied to the nuclear structure of the $^{90-98}$Zr isotopes. Accordingly, with respect to a $^{88}_{38}$Sr core, the empirical ^{92}Sr level scheme, representing the neutron degrees of freedom, together with ^{90}Zr, giving the proton degrees of freedom, were compared to the experimental levels of ^{94}Zr, as shown in Fig. 9; this figure is an updated version of Fig. 2 in Ref. [49]. The similarities between the ^{92}Sr+^{90}Zr and ^{94}Zr level schemes thus indicate that the proton-neutron part of the effective interaction in ^{94}Zr is either weak or state-independent [49]. The same result was obtained from a comparison of the ^{92}Zr level scheme to the empirical ^{90}Sr+^{90}Zr level schemes.

In ^{92}Zr the decay behavior of the 2_2^+ state at 1847.3 keV, identified as the one-phonon MS state, $2^+_{\rm ms}$, could not be described with the same approach as in its neighboring isotones, i.e., ^{94}Mo and ^{96}Ru, where ^{88}Sr had been used as the

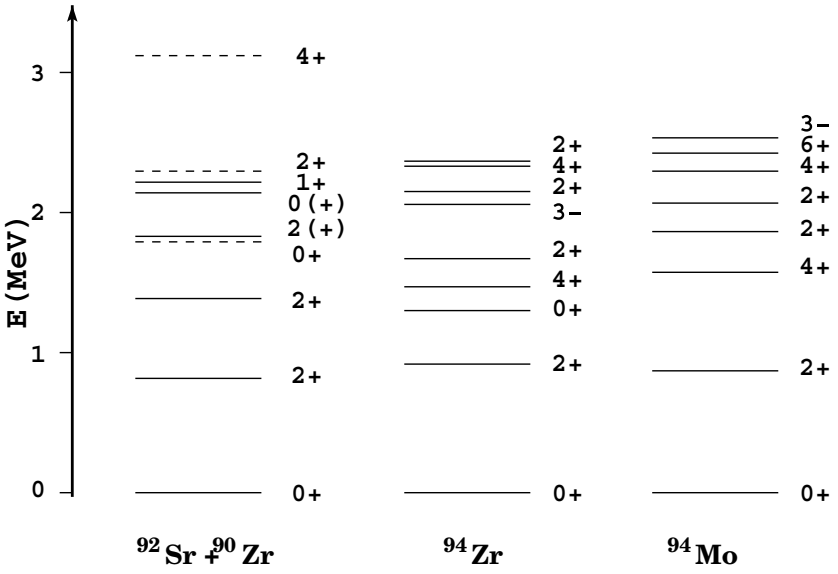

FIG. 9. Proton-neutron weak-coupling scheme for ^{94}Zr, as created from Fig. 2 in Ref. [49]. On the left, dashed lines represent ^{90}Zr levels and the solid lines represent ^{92}Sr; in the middle are ^{94}Zr levels. For comparison, the ^{94}Mo levels are shown on the right.

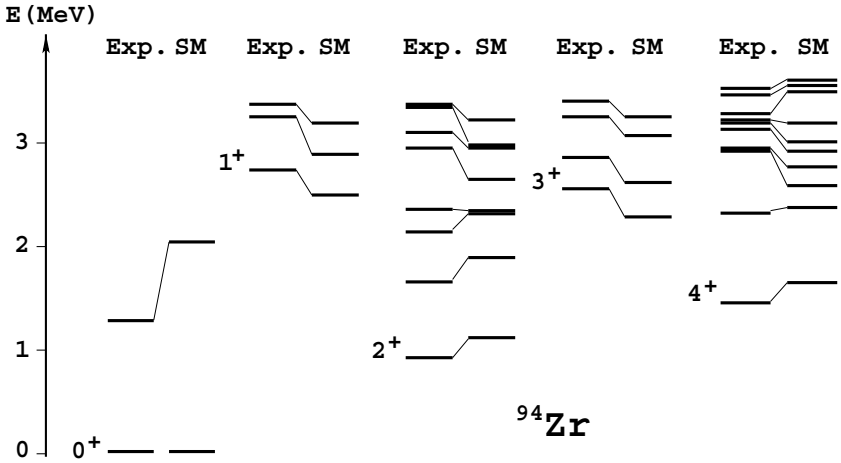

FIG. 10. The experimental and shell model calculation results for the low-lying states of ^{94}Zr.

core nucleus for model calculations [14,18]. It was concluded that the $2^+_{\rm ms}$ state in ^{92}Zr is not a pure MS state, due to subshell closure effects in the Zr isotopes (Ref. [19] and references therein). Consequently, it might be expected that in ^{94}Zr the 2^+_2 state at 1671.4 keV, identified as the one-phonon MS state, shows even less MS character; the $B(E2; 2^+_2 \rightarrow 0^+_1)$ value is larger than that in the neighboring nuclei and than the $2^+_1 \rightarrow 0^+_1$ transition. In ^{92}Zr, the $B(E2; 2^+_{\rm ms} \rightarrow 0^+_1)$ value is also large (see Table I). The g factors of the $2^+_{\rm ms}$ state in ^{92}Zr and the 2^+_2 state in ^{94}Zr have been recently measured [48]. The positive g factors, $g(2^+_2;^{94}\,{\rm Zr}) = +0.88(27)$ and $g(2^+_2;^{92}\,{\rm Zr}) = +0.76(50)$, indicate proton dominance in the wave functions, possibly contributing to the large $B(E2)$ values of their ground-state transitions. It is suggested [47] that the large positive g factors are a consequence of weak proton-neutron coupling combined with the $Z = 40$ subshell closure in these nuclei.

There is evidence of a neutron subshell closure, $N = 56$, in ^{96}Zr [3], which rapidly evolves to a shape-coexistence structure in ^{100}Zr [4]. In ^{96}Zr the first excited state, a 0^+ level at 1581 keV, along with the 2^+ state at 2225 keV and a 4^+ state at 2857 keV form a 4p-4h intruder-like band [3]. The proximity of ^{94}Zr to the subshell closures at $Z = 40$ and $N = 56$ is believed to play an important role in its nuclear structure.

C. Comparison to ^{94}Mo

Considering $^{88}_{38}{\rm Sr}_{50}$ as a core nucleus, ^{94}Zr and ^{94}Mo have the same numbers of valence nucleons: 2π-4ν for ^{94}Zr and 4π-2ν for ^{94}Mo. As an example of a nearly spherical collective nucleus, ^{94}Mo has been successfully described with several models [17]. The experimental level schemes of these two nuclei are compared in Fig. 9.

The yrast states in ^{94}Mo are mainly proton excitations [16]. For example, the g factor of the 2^+_1 state in ^{94}Mo is $+0.308(43)$ [49], indicating a dominant proton configuration, $\pi(g_{9/2})^2$, which has been confirmed by shell-model calculations [16]. As mentioned earlier, the g factor of the 2^+_2 state in ^{94}Zr has been recently measured [47] and its positive value also indicates proton dominance in the wave function. Also, another yrast state in ^{94}Mo exhibits similar transition rates to that of a the nonyrast state in ^{94}Zr, e.g., $B(E2; 4^+_1 \rightarrow 2^+_1) = 26(4)$ W.u. in ^{94}Mo [6] and the $B(E2; 4^+_2 \rightarrow 2^+_2) = 52^{+10}_{-8}$ W.u. in ^{94}Zr. These similarities could indicate that the 4^+_2 and 2^+_2 states in ^{94}Zr are similar to the 4^+_1 and 2^+_1 states in ^{94}Mo, which have dominant proton configurations. The low-lying states in ^{94}Zr, however, cannot be explained as simple collective excitations.

D. Configuration coexistence

The fact that in ^{94}Zr the transitions to the 2^+_1 and 2^+_2 states have different characteristics could be related to their different microscopic configurations. The configuration of the lowest 2^+ state at 918.8 keV is dominantly $\nu(d_{5/2})^4$ [49], which has been confirmed by its negative g factor, $-0.329(15)$ [37]. Two-neutron pick-up, $^{96}{\rm Zr}(p, t)^{94}{\rm Zr}$ [50], and two-neutron stripping, $^{92}{\rm Zr}(t, p)^{94}{\rm Zr}$ [51], reactions show that in ^{94}Zr the 2^+_2 level at 1671.4 keV is not populated as strongly as the 2^+_1 state A calculation for the $^{92}{\rm Zr}(t, p)^{94}{\rm Zr}$ reaction confirms that, indeed, the neutron contributions in these two states are different; the $\nu(3s_{1/2})$ orbit contributes more to the 2^+_2 state than to the 2^+_1 state [52]. As noted earlier, the wave function of the 2^+_2 state is mainly proton dominant.

It could be concluded that in ^{94}Zr there are two distinct configurations, i.e., the 2^+_1 and 2^+_2 states, to which other states decay through strong $E2$ transitions. The transitions with large $B(M1)$ values thus connect the states of one configuration to the states of the other configuration. An example of that is the $2^+_2 \rightarrow 2^+_1 M1$ transition, which connects the 2^+_2 state, a proton dominant excitation, to a neutron excitation, the 2^+_1 state.

E. Shell-model calculations

Shell-model calculations have been fairly successful in describing the binding energies, excitation energies, and transition rates between yrast states in ^{94}Zr (Refs. [45–47,52], and references therein). In the calculation of the $E2$ transition rates by Holt and coworkers [49], only the experimental $B(E2; 2^+_1 \rightarrow 0^+_1)$ and $B(E2; 4^+_1 \rightarrow 2^+_1)$ values could be

TABLE V. Single-particle energies used for ^{94}Zr shell-model calculations.

π	$(1p_{1/2})$	$(1g_{9/2})$	$(1g_{7/2})$	$(2d_{5/2})$	$(2d_{3/2})$	$(3s_{1/2})$
E_x(MeV)	−6.471	−6.162	2.500	2.500	2.500	2.500
ν	$(1g_{7/2})$	$(2d_{5/2})$	$(2d_{3/2})$	$(3s_{1/2})$	$(1h_{11/2})$	
E_x(MeV)	−4.885	−6.358	−4.350	−5.326	−3.300	

reproduced. The calculated $B(E2; 0_2^+ \rightarrow 2_1^+)$ value was far too small; $B(E2)_{\rm calc} = 0.01$ W.u. It was then concluded that this disagreement is attributed to configurations that are not accounted for in the calculations [49].

We performed new shell-model calculations for ^{94}Zr with the OXBASH code [53] using the $V_{\rm low-k}$ effective interaction described in Refs. [15,54]. The single-particle energies are listed in Table V, which also shows the model space. For valence protons, the $p_{1/2}$ single-particle energy was determined according to the first excited state in $^{93}_{39}$Y$_{54}$. This value is higher than that used for the $N = 52$ isotones, as is explained below.

The results of the calculations for the excitation energies of the low-lying states of ^{94}Zr are presented in Fig. 10, which indicates good correspondence between the experimental and calculated excitation energies, with the exception of the 0_2^+ state, with a 700-keV difference between the experimental and calculated values. The effective charges were adjusted to reproduce the experimental $B(E2; 2_1^+ \rightarrow 0_1^+)$, but could not reproduce the experimental $B(E2; 2_2^+ \rightarrow 0_1^+)$ value. The calculated results for some of the transition strengths are listed in Table VI.

Better agreement with the experimental $B(M1; 2_2^+ \rightarrow 2_1^+)$ value was achieved by changing the $\pi(p_{1/2})$ single-particle energy from −7.071 MeV to −6.471 MeV, which pushes the $p_{1/2}$ subshell to within 300 keV of the $g_{9/2}$ subshell. The result of the former value was $B(M1; 2_2^+ \rightarrow 2_1^+) = 0.025\ \mu_N^2$.

TABLE VI. Experimental data, taken from Table III, and spherical shell-model results calculated with the $V_{\rm low-k}$ interaction and ^{88}Sr core, for some of the low-lying states in ^{94}Zr; $e_p^{\rm eff} = 1.5\ e$, $e_n^{\rm eff} = 0.5\ e$, $g_p^l = 1$, $g_s^l = 0$, and a g^s quenching factor of $0.7(g_p^{s,\rm free} = 5.58$ and $g_n^{s,\rm free} = -3.82)$.

J_i	J_f	$B(M1)_{\rm Exp}$ (μ_N^2)	$B(E2)_{\rm Exp}$ (W.u.)	$B(M1)_{\rm SM}$ (μ_N^2)	$B(E2)_{\rm SM}$ (W.u.)
2_1^+	0_1^+		4.9(3)		5.5
4_1^+	2_1^+		0.878(23)		0.4
2_2^+	2_1^+	0.31(3)	0.18(2)	0.08	0.01
	0_1^+		7.8(7)		2.8
2_3^+	2_2^+	$0.07^{+0.04}_{-0.03}$	7^{+4}_{-3}	0.16	1.1
	2_1^+	$0.05^{+0.02}_{-0.01}$	11(3)	0.16	0.3
	0_1^+		$0.04^{+0.04}_{-0.02}$		2.9
2_4^+	2_2^+	$0.18^{+0.03}_{-0.02}$	1.02(15)	0.002	1.0
	0_2^+		6(1)		0.2
	2_1^+		$1.6^{+0.5}_{-0.4}$		2.4
4_2^+	2_2^+		52^{+10}_{-8}		2.0
	2_1^+		19^{+3}_{-2}		7.7

Raising the $\pi(p_{1/2})$ single-particle energy closer to that of the $\pi(1g_{9/2})$ indicates that $^{88}_{38}$Sr$_{50}$ is a better choice of a core nucleus for ^{94}Zr than ^{90}Zr.

The fact that these shell-model calculations and the earlier calculations by Holt *et al.* [49] were not successful in describing the transition strengths for the nonyrast states in ^{94}Zr could be indicative of the involvement of proton subshells other than $p_{1/2}$. It is evident that the subshell closure at $Z = 40$ and its proximity to the subshell closure at $N = 56$ in ^{94}Zr have an effect on the low-lying states, resulting in an unusual decay scheme for this nucleus. A shell-model calculation with a larger proton model space, including the $p_{3/2}$ and $f_{5/2}$ subshells, could be beneficial.

V. CONCLUSION

The low-lying states in ^{94}Zr were studied with the INS reaction. This study was initiated to search in ^{94}Zr for the one-phonon and multiphonon mixed-symmetry states, which have been seen in neighboring nuclei. The 2_2^+ state at 1671.4 keV was identified as the one-phonon MS state but with anomalous behavior [24]. Its $E2$ transition strength to the ground state is larger than that for the $2_1^+ \rightarrow 0_1^+$ transition. *To date, this is the only known example of such behavior*. Further analysis of ^{94}Zr resulted in even more anomalies and puzzling findings. The low-lying level scheme could not be described within a collective model, nor could it be entirely described with the proton-neutron weak-coupling scheme. The two-phonon quadrupole vibrational triplet could not be established, but candidates for members of the $(2_1^+ \otimes 3_1^-)$ quintplet have been suggested. A classification of the positive-parity states based on their decay patterns was established and simple interpretations proposed. The difference in the decay patterns of the excited states populating the 2_1^+ state and those decaying to the 2_2^+ state could indicate a sort of configuration coexistence, possibly attributed to core excitations.

It is difficult to understand the nuclear structure of ^{94}Zr based on these experimental results. Shell-model calculations were not successful in describing the $E2$ transition rates for decays from the 2_2^+ and 2_1^+ states simultaneously.

ACKNOWLEDGMENTS

The authors are pleased to acknowledge Gene Baber for technical support at the University of Kentucky accelerator facility. The contributions of B. Crider, who provided some of the new sorting codes for singles data analysis; D. Weisshaar, who provided parts of the com-

puter software for coincidence data analysis; and J. D. Holt, who provided the $V_{\mathrm{low-k}}$ effective interaction for theoretical calculations. Fruitful disscussion with V. Werner and N. Benczer-Koller are acknowledged. This material is based on work supported by the US National Science Foundation under grant no. PHY-0652415. The experiments at TUNL were supported by US Department of Energy under grants DE-FG02-03ER41231, DE-FG02-97ER41041, and DE-FG02-97ER41042.

[1] F. Schussler, J. A. Pinston, E. Monnand, A. Moussa, G. Jung, E. Koglin, B. Pfeiffer, R. V. F. Janssens, and J. van Klinken, Nucl. Phys. **A339**, 415 (1980).
[2] P. E. Garrett, W. Younes, J. A. Becker, L. A. Bernstein, E. M. Baum, D. P. DiPrete, R. A. Gatenby, E. L. Johnson, C. A. McGrath, S. W. Yates, M. Devlin, N. Fotiades, R. O. Nelson, and B. A. Brown, Phys. Rev. C **68**, 024312 (2003).
[3] G. Molnár, T. Belgya, B. Fazekas, Á. Veres, S. W. Yates, E. L. Kleppinger, R. A. Gatenby, R. Julin, J. Kumpulainen, A. Passoja, and E. Verho, Nucl. Phys. **A500**, 43 (1989).
[4] H. Mach, M. Moszynski, R. L. Gill, F. K. Wohn, J. A. Winger, John C. Hill, G. Molnár, and K. Sistemich, Phys. Lett. **B230**, 21 (1989).
[5] G. Lhersonnaeu, B. Pfeiffer, K.-L. Kratz, T. Enqvist, P. P. Jauho, A. Jokinen, J. Kantele, M. Leino, J. M. Parmonen, H. Penttilä, and J. Äystö, Phys. Rev. C **49**, 1379 (1994).
[6] N. Pietralla, C. Fransen, D. Belic, P. von Brentano, C. Friessner, U. Kneissl, A. Linnemann, A. Nord, H. H. Pitz, T. Otsuka, I. Schneider, V. Werner, and I. Wiedenhöver, Phys. Rev. Lett. **83**, 1303 (1999).
[7] C. Fransen, N. Pietralla, Z. Ammar, D. Bandyopadhyay, N. Boukharouba, P. von Brentano, A. Dewald, J. Gableske, A. Gade, J. Jolie, U. Kneissl, S. R. Lesher, A. F. Lisetskiy, M. T. McEllistrem, M. Merrick, H. H. Pitz, N. Warr, V. Werner, and S. W. Yates, Phys. Rev. C **67**, 024307 (2003).
[8] A. Arima and F. Iachello, Ann. Rev. Nucl. Part. Sci. **31**, 75 (1981).
[9] F. Iachello, Phys. Rev. Lett. **53**, 1427 (1984).
[10] A. Faessler, Nucl. Phys. **A85**, 653 (1966).
[11] G. Siems, U. Neuneyer, I. Wiedenhöver, S. Albers, M. Eschenauer, R. Wirowski, A. Gelberg, P. von Brentano, and T. Otsuka, Phys. Lett. **B320**, 1 (1994).
[12] N. Pietralla, C. J. Barton, R. Krücken, C. W. Beausang, M. A. Caprio, R. F. Casten, J. R. Cooper, A. A. Hecht, H. Newman, J. R. Novak, and N. V. Zamfir, Phys. Rev. C **64**, 031301 (2001).
[13] H. Klein, A. F. Lisetskiy, N. Pietralla, C. Fransen, A. Gade, and P. von Brentano, Phys. Rev. C **65**, 044315 (2002).
[14] C. Fransen, V. Werner, D. Bandyopadhyay, N. Boukharouba, S. R. Lesher, M. T. McEllistrem, J. Jolie, N. Pietralla, P. von Brentano, and S. W. Yates, Phys. Rev. C **71**, 054304 (2005).
[15] J. N. Orce, J. D. Holt, A. Linnemann, C. J. McKay, S. R. Lesher, C. Fransen, J. W. Holt, A. Kumar, N. Warr, V. Werner, J. Jolie, T. T. S. Kuo, M. T. McEllistrem, N. Pietralla, and S. W. Yates, Phys. Rev. Lett. **97**, 062504 (2006).
[16] A. F. Lisetskiy, N. Pietralla, C. Fransen, R. V. Jolos, and P. von Brentano, Nucl. Phys. **A677**, 100 (2000).
[17] N. Lo Iudice and Ch. Stoyanov, Phys. Rev. C **65**, 064304 (2002).
[18] V. Werner, D. Belic, P. von Brentano, C. Fransen, A. Gade, H. von Garrel, J. Jolie, U. Kneissl, C. Kohstall, A. Linnemann, A. F. Lisetskiy, N. Pietralla, H. H. Pitz, M. Scheck, K. H. Speidel, F. Stedile, and S. W. Yates, Phys. Lett. **B550**, 140 (2002).
[19] N. Pietralla, P. von Brentano, and A. F. Lisetskiy, Prog. Part. Nucl. Phys. **60**, 225 (2008).
[20] S. R. Lesher, C. J. McKay, M. Mynk, D. Bandyopadhyay, N. Boukharouba, C. Fransen, J. N. Orce, M. T. McEllistrem, and S. W. Yates, Phys. Rev. C **75**, 034318 (2007).
[21] D. Abriola and A. A. Sonzogni, Nucl. Data Sheets **107**, 2423 (2006).
[22] http://www.nndc.bnl.gov. (*NNDC database*).
[23] G. P. Glasgow, F. D. McDaniel, J. L. Weil, J. D. Brandenberger, and M. T. McEllistrem, Phys. Rev. C **18**, 2520 (1978).
[24] E. Elhami, J. N. Orce, S. Mukhopadhyay, S. N. Choudry, M. Scheck, M. T. McEllistrem, and S. W. Yates, Phys. Rev. C **75**, 011301(R) (2007).
[25] P. E. Garrett, N. Warr, and S. W. Yates, J. Res. Natl. Inst. Stand. Technol. **105**, 141 (2000).
[26] A. Hutcheson, C. T. Angell, J. A. Becker, M. Boswell, A. S. Crowell, D. Dashdorj, B. Fallin, N. Fotiades, C. R. Howell, H. J. Karwowski, J. H. Kelley, M. Kiser, R. A. Marci, R. O. Nelson, R. S. Pedroni, A. P. Tonchev, W. Tornow, D. J. Vieira, G. J. Weisel, and J. B. Wilhelmy, Nucl. Instrum. Methods B **261**, 369 (2007).
[27] R. Fox, C. Bolen, K. Orji, and J. Venema, NSCLSpecTcl Meeting the Needs of Preliminary Nuclear Physics Data Analysis, 11th Annual Tcl/Tk Conference, New Orleans, LA USA (2004).
[28] J. Theuerkauf, S. Esser, S. Krink, M. Luig, N. Nicolay, O. Stuch, and H. Wolters, computer code TV (unpublished), http://www.ikp.uni-koeln.de/∼fitz (1993).
[29] E. Elhami, Ph.D. Dissertation, University of Kentucky (2008).
[30] E. Sheldon and V. C. Rogers, Comput. Phys. Commun. **6**, 99 (1973); P. A. Moldauer, Phys. Rev. C **14**, 764 (1976).
[31] R. M. Diamond, E. Matthias, J. O. Newton, and F. S. Stephens, Phys. Rev. Lett. **16**, 1205 (1966).
[32] E. Sheldon and D. M. Van Patter, Rev. Mod. Phys. **38**, 143 (1966).
[33] T. Belgya, G. Molnár, and S. W. Yates, Nucl. Phys. **A607**, 43 (1996).
[34] A. E. Blaugrund, Nucl. Phys. **88**, 501 (1966).
[35] K. B. Winterbon, Nucl. Phys. **A246**, 293 (1975).
[36] G. Jakob, N. Benczer-Koller, J. Holden, G. Kumbartzki, T. J. Mertzimekis, K.-H. Speidel, C. W. Beausang, and R. Krücken, Phys. Lett. **B468**, 13 (1999).
[37] H. J. Rose and D. M. Brink, Rev. Mod. Phys. **39**, 306 (1967).
[38] V. Werner, Ph.D. Dissertation, Universität zu Köln (2004).
[39] C. Fransen, Universität zu Köln (private communication).
[40] E. Frota-Pessoa and S. Joffily, Nuovo Cimento A **96**, 347 (1986).
[41] J. N. Orce, S. N. Choudry, B. Crider, E. Elhami, S. Mukhopadhyay, M. Scheck, M. T. McEllistrem, and S. W. Yates, Phys. Rev. C **77**, 029902(E) (2008).
[42] D. Pantelica, I. Gh. Stefan, N. Nica, M.-G. Porquet, G. Duchene, A. Astier, S. Courtin, I. Deloncle, F. Hoellinger, A. Bauchet, N. Buforn, L. Donadille, O. Dorvaux, J. Duprat, B. J. P. Gall, C. Gautherin, T. Kutsarova, S. Lalkovski, R. Lucas, M. Meyer, A. Minkova, A. Prvost, N. Redon, N. Schulz, H. Sergolle, O. Stézowski, Ts. Venkova, and A. Wilson, Phys. Rev. C **72**, 024304 (2005).

[43] A. Kumar, J. N. Orce, S. R. Lesher, C. J. McKay, M. T. McEllistrem, and S. W. Yates, Phys. Rev. C **72**, 034313 (2005).
[44] W. Andrejtscheff, C. Kohstall, P. von Brentano, C. Fransen, U. Kneissl, N. Pietralla, and H. H. Pitz, Phys. Lett. **B506**, 239 (2001).
[45] I. Talmi, Phys. Rev. **126**, 2116 (1962).
[46] A. Holt, T. Engeland, M. Hjorth-Jensen, and E. Osnes, Phys. Rev. C **61**, 064318 (2000).
[47] H. Mach, E. K. Warburton, W. Krips, R. L. Gill, and M. Moszyński, Phys. Rev. C **42**, 568 (1990).
[48] V. Werner, N. Benczer-Koller, G. Kumbartzki, J. D. Holt, P. Boutachkov, E. Stefanova, M. Perry, N. Pietralla, H. Ai, K. Aleksandrova, G. Anderson, R. B. Cakirli, R. J. Casperson, R. F. Casten, M. Chamberlain, C. Copos, B. Darakcheva, S. Eckel, M. Evtimova, C. R. Fitzpatrick, A. B. Garnsworthy, G. Gürdal, A. Heinz, D. Kovacheva, C. Lambie-Hanson, X. Liang, P. Manchev, E. A. McCutchan, D. A. Meyer, J. Qian, A. Schmidt, N. J. Thompson, E. Williams, and R. Winkler, Phys. Rev. C **78**, 031301(R) (2008).
[49] P. F. Mantica, A. E. Stuchbery, D. E. Groh, J. I. Prisciandaro, and M. P. Robinson, Phys. Rev. C **63**, 034312 (2001).
[50] J. B. Ball, R. L. Auble, and P. G. Roos, Phys. Rev. C **4**, 196 (1971).
[51] E. R. Flynn, J. G. Beery, and A. G. Blair, Nucl. Phys. **A218**, 285 (1974).
[52] C. Zhang, S. Wang, and J. Gu, Phys. Rev. C **60**, 054316 (1999).
[53] B. A. Brown, A. Etchegoyen, N. S. Godwin, W. D. M. Rae, W. A. Richter, W. E. Ormand, E. K. Warburton, J. S. Winfield, L. Zhao, and C. H. Zimmerman, MSU-NSCL Report No. 1289.
[54] J. D. Holt, N. Pietralla, J. W. Holt, T. T. S. Kuo, and G. Rainovski, Phys. Rev. C **76**, 034325 (2007).